Layer-by-Layer Assembly of Titania Nanosheet/Polycation Composite Films

Takayoshi Sasaki,* Yasuo Ebina, Tomohiro Tanaka, Masaru Harada, and Mamoru Watanabe

Advanced Materials Laboratory, National Institute for Materials Science, 1-1 Namiki, Tsukuba, Ibaraki 305-0044, Japan

Gero Decher

Université Louis Pasteur and CNRS, Institut Charles Sadron, 6, rue Boussingault, F-67083 Strasbourg Cedex, France

Received May 16, 2001. Revised Manuscript Received August 20, 2001

Unilamellar titania crystallites of $Ti_{1-\delta}O_2^{4\delta-}$ ($\delta = 0.0875$) and polydiallyldimethylammonium chloride have been alternately deposited layer-by-layer onto various substrates from their aqueous media. An atomic force microscopy (AFM) image visualized the adsorbed nanosheets, which gave efficient coverage of the substrate surface. The resulting multilayer film apparently displayed a very intense UV absorption ($\epsilon = 2.2 \times 10^4$ mol^{-1} dm^3 cm^{-1} at 265 nm) due to the titania nanosheets with a molecular thickness. X-ray diffraction (XRD) measurements detected a Bragg peak, which reflects a nanosheet/polycation nanostructure inside the film. Its multilayer repeat distance was 1.4−1.7 nm, being dependent on the surrounding humidity. Simulation on the XRD profile suggested that the obtained films have some structural disorder, involving about 20% of the mean displacement for the multilayer repeat spacing. Spectroscopic ellipsometry data can successfully be analyzed based on a multilayer assembly model composed of titania nanosheets that are ∼1.2 nm thick and polycations that are ∼0.7 nm thick, which is substantially compatible with the XRD and AFM data.

Introduction

The sequential adsorption procedure was originally developed for the fabrication of multilayer films of polymers.[1] The technique is based on the alternate adsorption of polycation and polyanion monolayers from their aqueous solutions. This simple procedure enables the layer-by-layer growth of films and the control of their thickness with a nanometer-scale precision.

Its simple principle, of self-assembly of oppositely charged polyelectrolytes, is applicable to a wide variety of materials besides organic macromolecules.[1,2] One of the most prominent highlights is the design of a bioreactor membrane by the assembly of different kinds of enzymatic proteins.[3] It has been demonstrated that one can control the metabolism function of the film by arranging the proteins in different sequences.

This technique is also of great importance in the field of inorganic material science, providing a rational route to design new nanostructured systems. A wide range of inorganic materials, typically colloidal nanoparticles and clusters, have been assembled with appropriate polymers to produce nanocomposite multilayer films.[2] In addition to them, lamellar crystallites, obtained by exfoliating layered crystals, have also been incorporated as building blocks of multilayer assemblies. The most typical example is smectite clay minerals which spontaneously undergo infinite swelling in water.[4] Apart from them, various layered compounds have been delaminated into their colloidal single sheets via soft-chemical treatments, e.g., the action of bulky surfactants.[5] The resulting unilamellar crystallites, which can be described as nanosheets, are attractive for several reasons: (i) ultimate two-dimensionality with the thickness of subnano- to nanometer range, (ii) high crystallinity and well-defined composition, and (iii) novel or enhanced physical properties. These features have stimulated great interest in the fabrication of their thin

* To whom correspondence should be addressed. E-mail: sasaki.takayoshi@nims.go.jp. Fax: +81-298-54-9061.

(1) (a) Decher, G. Layered Nanoarchitectures via Directed Assembly of Anionic and Cationic Molecules. In *Comprehensive Supramolecular Chemistry, Templating, Self-Assembly and Self-Organization*; Sauvage, J. P., Hosseini, M. W., Eds.; Pergamon Press: Oxford, 1996; Vol. 9, pp 507−528. (b) Decher, G. *Science* **1997**, 277, 1232.

(2) Fendler, J. H. *Chem. Mater.* **1996**, *8*, 1616.

(3) (a) Lvov, Y.; Ariga, K.; Ichinose, I.; Kunitake, T. *J. Am. Chem. Soc.* **1995**, *117*, 6117. (b) Onda, M.; Lvov, Y.; Ariga, K.; Kunitake, T. *Biotechnol. Bioeng.* **1996**, *51*, 163. (c) Sun, Y.; Zhang, X.; Sun, C.; Wang, B.; Shen, J. *Macromol. Chem. Phys.* **1996**, *197*, 147.

(4) (a) Kleinfeld, E. R.; Ferguson, G. S. *Science* **1994**, *265*, 370. (b) Kleinfeld, E. R.; Ferguson, G. S. *Chem. Mater.* **1995**, *7*, 2327. (c) Lvov, Y.; Ariga, K.; Ichinose, I.; Kunitake, T. *Langmuir* **1996**, *12*, 3038. (d) Laschewsky, A.; Wischerhoff, E.; Kauranen, M.; Persoons, A. *Macromolecules* **1997**, *30*, 8304. (e) Kotov, N. A.; Haraszti, T.; Turi, L.; Zavala, G.; Geer, R. E.; Dékány, I.; Fendler, J. H. *J. Am. Chem. Soc.* **1997**, *119*, 6821. (f) Kotov, N. A.; Magonov, S.; Tropsha, E. *Chem. Mater.* **1998**, *10*, 886. (g) Van Duffel, B.; Schoonheydt, R. A.; Grim, C. P. M.; De Schryver, F. C. *Langmuir* **1999**, *15*, 7520. (h) Rouse, J. H.; MacNeill, B. A.; Ferguson, G. S. *Chem. Mater.* **2000**, *12*, 2502. (i) Kim, D. W.; Blumstein, A.; Kumar, J.; Tripathy, S. K. *Chem. Mater.* **2001**, *13*, 243.

(5) (a) Jacobson, A. J. *Mater. Sci. Forum* **1994**, *152−153*, 1. (b) Jacobson, A. J. In *Comprehensive Supramolecular Chemistry*; Alberti, G., Bein, T., Eds.; Elsevier Science: Oxford, U.K., 1996; Vol. 7, pp 315−335.

10.1021/cm010478h CCC: $20.00
Published on Web 11/09/2001

films. Actually, a number of nanosheet crystallites obtained from zirconium phosphates,[6] niobates,[7] titanoniobates,[6,7] layered perovskites,[7,8] and graphite oxide[9] have been incorporated into films.

Titanium oxides have attracted considerable attention owing to their usefulness in terms of optical properties and photocatalytic activities.[10] Recently, several groups have reported ultrathin films with titania nanoparticles grown via sequential adsorption.[11] On the other hand, we have demonstrated that a layered titanate can be delaminated into its molecular single sheets.[12] The resultant nanosheets having a composition of $Ti_{1-\delta}O_2^{4\delta-}$ exhibit distinctive physicochemical properties in comparison with extensively studied titania nanoparticles. For example, the nanosheet crystallites show UV−vis spectra which are characterized by their sharp and prominent peak as well as the large blue-shift of the absorption edge.[13] Thus, it is of great interest and importance to assemble the titania nanosheets layer-by-layer to produce a nanostructured ultrathin film. Here, we report the stepwise construction of multilayer assemblies of titania nanosheets and polycations and their characterizations mainly from optical and structural points of view.[14]

Results and Discussion

Formation of the Multilayer Films. Transparent films were obtained by alternately dipping a substrate in a colloidal suspension of the titania nanosheets and a polydiallyldimethylammonium (PDDA) solution. To have a cationic surface, the substrate was precoated with polyethylenimine (PEI). In the layer-by-layer deposition process, the substrate surface became very hydrophobic after immersion in the titania suspension.

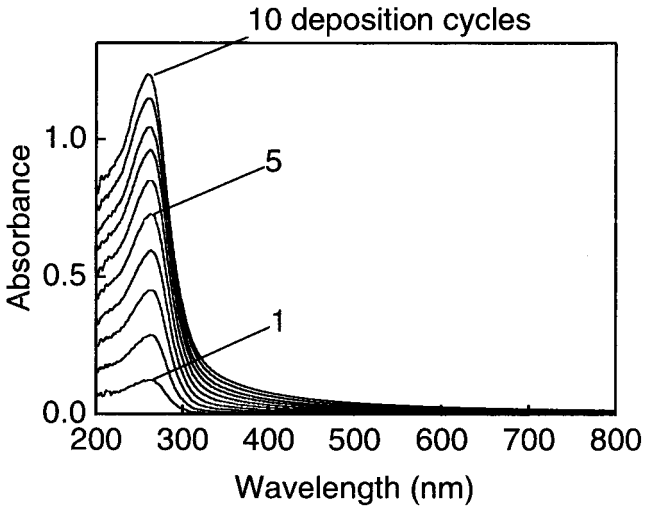

Figure 1. UV−vis absorption spectra in the multilayer buildup process. Experimental conditions employed for this film growth: deposition time of 20 min and nanosheet concentration of 0.08 g dm^{-3}.

This may be due to the adsorption of tetrabutylammonium (TBA) ions on top of the titania nanosheets, which were present in the suspension as counterions. The hydrophobic surface gradually turned into a hydrophilic one by washing with copious water. This careful rinsing is important; otherwise, the film tended to become heterogeneous giving a visibly discernible stain on its surface.

The multilayer buildup process was monitored with a UV−vis spectrum of the film after each deposition cycle as depicted in Figure 1. The spectral profile having a peak at 265 nm was similar to that of the titania nanosheet dispersed in a colloidal suspension.[13] The only difference was a higher baseline in the visible light region, which may be attributable to reflectance by the nanosheet crystallites on the film surface, as will be described below. The polycations such as PDDA and PEI do not have absorption in this spectral range. Thus, a nearly linear enhancement in peak-top absorbance provides persuasive evidence for the regular growth of the multilayer assembly.

There are many deposition parameters to be examined in the preparation of a high quality film. Because the adsorption of PDDA has been examined and conditions to obtain its monolayer coverage have been established, most typical deposition parameters in the literatures were used as indicated in the Experimental Section. In this study, adsorption behaviors of the titania nanosheets were examined to obtain a deposited layer of densely tiled nanosheets. The effect of the nanosheet concentration is depicted in Figure 2 as one of such examples. There is a tendency for the absorbance to increase with increase in the concentration used in the nanosheet deposition. But there was no appreciable increment above 0.08 g dm^{-3}, suggesting a saturation of adsorption. If the deposition time was protracted, the saturated loading at a similar level was achieved even at lower concentrations. This saturation may be accounted for by the principle of electrostatic self-assembly. Full coverage of the substrate surface with nanosheet crystallites brings about charge reversal, which prevents further adsorption.

(6) (a) Keller, S. W.; Kim, H.-N.; Mallouk, T. E. *J. Am. Chem. Soc.* **1994**, *116*, 8817. (b) Kim, H.-N.; Keller, S. W.; Mallouk, T. E.; Schmitt, J.; Decher, G. *Chem. Mater.* **1997**, *9*, 1414. (c) Kaschak, D. M.; Johnson, S. A.; Hooks, D. E.; Kim, H.-N.; Ward, M. D.; Mallouk, T. E. *J. Am. Chem. Soc.* **1998**, *120*, 10887. (d) Kerimo, J.; Adams, D. M.; Barbara, P. F.; Kaschak, D. M.; Mallouk, T. E. *J. Phys. Chem. B* **1998**, *102*, 9451.

(7) Fang, M.; Kim, C. H.; Saupe, G. B.; Kim, H.-N.; Waraksa, C. C.; Miwa, T.; Fujishima, A.; Mallouk, T. E. *Chem. Mater.* **1999**, *11*, 1526.

(8) (a) Kaschak, D. M.; Lean, J. T.; Waraksa, C. C.; Saupe, G. B.; Usami, H.; Mallouk, T. E. *J. Am. Chem. Soc.* **1999**, *121*, 3435. (b) Schaak, R. E.; Mallouk, T. E. *Chem. Mater.* **2000**, *12*, 2513. (c) Schaak, R. E.; Mallouk, T. E. *Chem. Mater.* **2000**, *12*, 3427.

(9) (a) Kotov, N. A.; Dékány, I.; Fendler, J. H. *Adv. Mater.* (*Weinheim, Ger.*) **1996**, *8*, 637. (b) Cassagneau, T.; Fendler, J. H. *Adv. Mater.* (*Weinheim, Ger.*) **1998**, *10*, 877. (c) Kovtyukhova, N. I.; Ollivier, P. J.; Martin, B. R.; Mallouk, T. E.; Chizhik, S. A.; Buzaneva, E. V.; Gorchinskiy, A. D. *Chem. Mater.* **1999**, *11*, 771.

(10) (a) Hagfeldt, A.; Grätzel, M. *Chem. Rev.* **1995**, *95*, 49. (b) Grätzel, M. Nanocrystalline Electronic Junctions. In *Semiconductor Nanoclusters: Physical, Chemical, and Catalytic Aspects*; Kumat, P. V., Meisel, D., Eds.; Elsevier: Amsterdam, 1996; Vol. 103; pp 353−375. (c) Kumat, P. V. *Native and Surface Modified Semiconductor Nanoclusters*; Kumat, P. V., Ed.; John Wiley & Sons: New York, 1997; Vol. 44, pp 273−343.

(11) (a) Kotov, N. A.; Dékány, I.; Fendler, J. H. *J. Phys. Chem.* **1995**, *99*, 13065. (b) Liu, Y.; Wang, A.; Claus, R. *J. Phys. Chem. B* **1997**, *101*, 1385. (c) Kovtyukhova, N.; Ollivier, P. J.; Chizhik, S.; Dubravin, A.; Buzaneva, E.; Gorchinskiy, A.; Marchenko, A.; Smirnova, N. *Thin Solid Films* **1999**, *337*, 166. (d) Cassagneau, T.; Fendler, J. H.; Mallouk, T. E. *Langmuir* **2000**, *16*, 241.

(12) (a) Sasaki, T.; Watanabe, M.; Hashizume, H.; Yamada, H.; Nakazawa, H. *J. Am. Chem. Soc.* **1996**, *118*, 8329. (b) Sasaki, T.; Watanabe, M. *J. Am. Chem. Soc.* **1998**, *120*, 4682.

(13) Sasaki, T.; Watanabe, M. *J. Phys. Chem. B* **1997**, *101*, 10159.

(14) Sasaki, T.; Ebina, Y.; Watanabe, M.; Decher, G. *Chem. Commun.* **2000**, 2163.

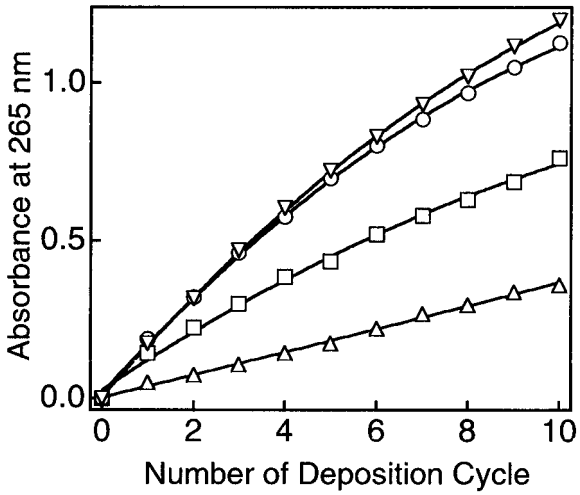

Figure 2. Peak-top absorbance as a function of deposition cycle. Symbols such as triangle, square, circle, and inversed triangle represent the data for the films prepared at the nanosheet concentration of 0.02, 0.04, 0.08, and 0.16 g dm^{-3}, respectively. The deposition time was 20 min for all the cases.

Figure 3 shows tapping mode atomic force microscope (AFM) images of the film after the first deposition of the titania nanosheets at two typical loadings. The surface was densely covered with the nanosheet crystallites of sub-micron in lateral size. Their thickness was 1.2−1.3 nm, which confirms that the unilamellar crystallites were adsorbed.[15] In addition to the monolayer of the nanosheets, there were some overlapped patches and gaps between the crystallites. In reflection of this topography, the height profile of the image revealed three discrete peaks attributable to the uncovered surface, monolayer, and overlapped nanosheets, although they were not well-resolved. We estimated their population by peak deconvolution, the results of which are summarized in Table 1. The film at the saturated loading of the nanosheets showed a total coverage of ∼90%. The overlap of the nanosheets also increased as the coverage became higher. This may be inevitable for the film with nanosheet crystallites with large lateral dimensions, such as several hundred nanometers in this case. The nanosheets are adhered to the oppositely charged surface, but there should be an increasing possibility of overlap with decreasing bare cationic surface. In this study, mainly the films at the saturated loading were characterized, which will be described below.

Optical Properties. The film showed an average enhancement of absorbance of 0.064 per layer pair at 265 nm (see Figure 1).[16] This UV-light absorbability is higher in comparison with multilayer films of titania nanoparticles assembled with appropriate polymers via the consecutive adsorption technique.[11] The two-dimensional nature with an ultrathin thickness of ∼1 nm may be responsible for the pronounced UV absorption.

If the substrate surface is completely covered with a monolayer of the titania nanosheets, the adsorbed amount can be calculated to be 2.2×10^{-7} g cm^{-2} (= $2 \times M_w/N_a \times S_{uc}$) where M_w, N_a, and S_{uc} represent the formula weight of $Ti_{1-\delta}O_2^{4\delta-}$ (= 75.7 for $\delta = 0.0875$), Avogadro number, and two-dimensional unit cell area for the nanosheet (= 0.114 (= 0.38 × 0.30) nm^2). Multiplication by 2 is needed since a "two-dimensional unit cell" contains two formula units of $Ti_{1-\delta}O_2^{4\delta-}$.[15] Accordingly, an apparent molar extinction coefficient of the film is estimated to be 2.2×10^4 mol^{-1} dm^3 cm^{-1}.

The colloidal suspension of the titania nanosheets shows Lambert−Beer behavior.[13] An absorbance of 1.5 was observed at 265 nm for the nanosheet content of

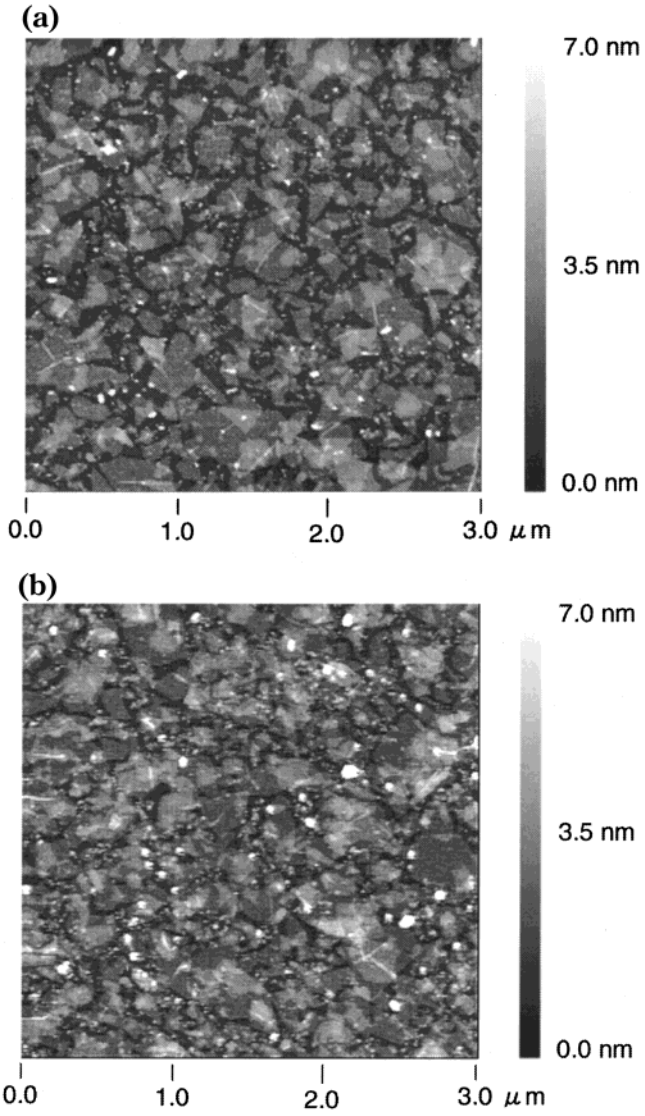

Figure 3. Tapping mode AFM images of the first titania-nanosheet layer on a PEI-coated Si wafer. Nanosheet concentration: (a) 0.04 g dm^{-3} and (b) 0.08 g dm^{-3}. Deposition time was 20 min.

Table 1. Surface Topography of the First Layer of the Titania Nanosheets Deposited onto the PEI-Coated Si Wafer

concn[a] (g dm^{-3})	surface coverage[b] (%)	overlapped area[b] (%)
0.02	45(6)	7(1)
0.04	71(4)	23(3)
0.08	88(2)	42(4)
0.16	91(2)	48(7)

[a] The nanosheet content in the colloidal suspension. [b] The averaged value for 10 different images (3 × 3 μm^2). The numeral in parentheses denotes the standard deviation.

(15) Sasaki, T.; Ebina, Y.; Kitami, Y.; Watanabe, M.; Oikawa, T. *J. Phys. Chem. B* **2001**, *105*, 6116.

(16) The observed absorbance shown in Figure 1 should be divided by 2, thus taking into account films on both sides of quartz substrate.

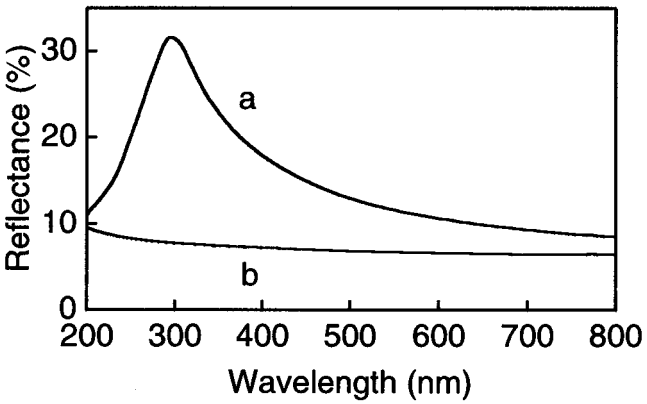

Figure 4. Reflectance spectra: (a) the multilayer film of PEI/$Ti_{1-\delta}O_2^{4\delta-}$/(PDDA/$Ti_{1-\delta}O_2^{4\delta-}$)$_9$ on quartz glass and (b) the substrate itself.

1.05×10^{-2} g dm^{-3}, which corresponds to a molar extinction coefficient, ϵ, of 1.2×10^4 mol^{-1} dm^3 cm^{-1}. This is approximately half of that obtained for the film. This discrepancy between calculated and experimental data does not necessarily indicate that more than a single monolayer of the titania nanosheets is deposited in one adsorption reaction. The difference may rather be accounted for by the high reflectivity of the film or by the anisotropic UV-ray absorption by the nanosheet crystallite. In the film, the nanosheets are deposited with their two-dimensional face parallel to the substrate while they are randomly oriented in the suspension.

The first possibility was examined by measuring a reflectance spectrum of the sample with ten-layered films on both sides of the quartz glass (see Figure 4), for which absorption spectra were measured in Figure 1. A reflectivity of 25.0% was observed at 265 nm where the absorption peak exists. The genuine optical absorption, *A*, by the titania nanosheets can be deduced from the following relationship

$$T = 100 - R - A \qquad (1)$$

where *T* and *R* are percentage transmittance and percentage reflectivity, respectively.[17] Since transmittance at 265 nm for the sample was 5.3%, as converted from the apparent absorbance of 1.27 in Figure 1, the optical absorption, *A*, is estimated to be 69.7% or 0.52 in absorbance. As noted above, if the titania nanosheets form a perfect monolayer without gaps and overlaps on each adsorption, 20 of their layers weigh 4.4×10^{-6} g cm^{-2}. It is expected that this amount of the nanosheets should give the optical density of 0.63 by using the molar extinction coefficient deduced from the colloidal suspension. This value seems to be in good accord with the observed data of 0.52 when the accuracy of this approximate calculation is considered. However, by taking the AFM data into account (Table 1) that the first deposited layer of the nanosheets was more than a perfect monolayer by ~30% (88% for monolayer + 42% for overlapped layer), the discrepancy is enlarged. If this is true for the nanosheet layers after the second deposition, the film contains 5.7×10^{-6} g of the nanosheets per cm^2, which should show the absorbance of 0.82. The second possibility, that is the anisotropic optical properties of the nanosheet, may explain this difference. Such a study is now underway.

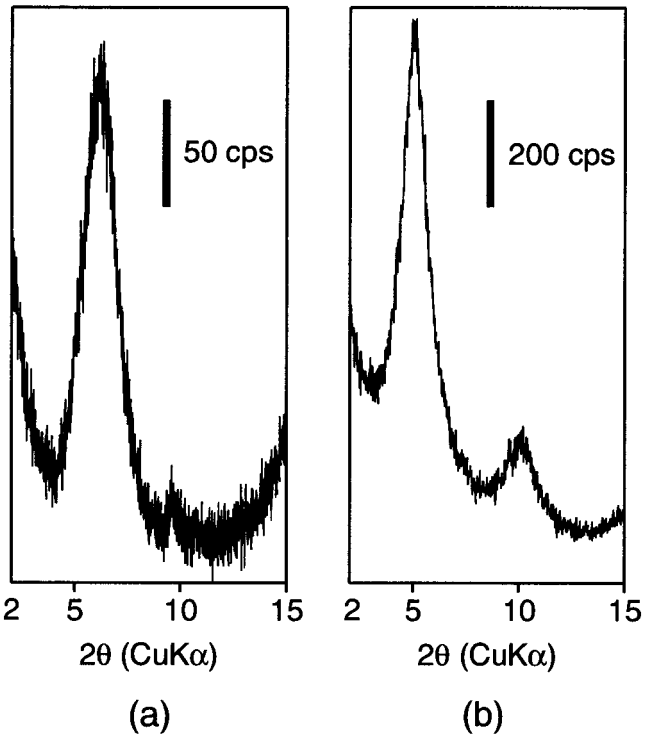

Figure 5. XRD patterns for (a) the multilayer assembly of PEI/$Ti_{1-\delta}O_2^{4\delta-}$/(PDDA/$Ti_{1-\delta}O_2^{4\delta-}$)$_9$ on quartz glass and (b) a comparable nanocomposite powder prepared via flocculation.

Multilayer Nanostructure. A Bragg peak showing an interplanar spacing of 1.4−1.7 nm appeared, as depicted by Figure 5a. This diffraction peak can be ascribed to a repeating pair of $Ti_{1-\delta}O_2^{4\delta-}$/PDDA. Its progressive increase in intensity was observed with increase in the deposition cycle,[14] which also supports the layer-by-layer electrostatic self-assembly. It is interesting to compare this profile with that for a $Ti_{1-\delta}O_2^{4\delta-}$/PDDA nanocomposite prepared in bulk. The slow addition of the PDDA solution into the titania suspension spontaneously induced flocculation to produce a lamellar nanocomposite in which the polycation is accommodated in the titanate gallery. Their synthesis will be described elsewhere.[18] The flocculated product had a relatively higher crystallinity, showing sharper basal reflections up to several higher order lines. This may be ascribed to a larger stacking number and a smaller lattice strain. These may be achieved by free growth conditions for the bulk material.

The multilayer repeat distance was dependent on the drying conditions. A relatively large value of ~1.7 nm was observed just after the preparation, while it decreased to a constant value of 1.4 nm when the film was aged under N_2 gas flow for several days. This shrinkage is due to the dehydration of the film, which was found to be reversible, as shown by Figure 6. The interlayer expansion−contraction of 0.3 nm suggests the insertion−removal of a monolayer of H_2O molecules. Ferguson and co-workers[4b] have reported a similar hydration−dehydration reaction for a multilayer film of montmorillonite sheets and PDDA, which takes place within seconds. In contrast, the titania film in the present

(17) Light scattering is ignored.

(18) Unpublished data.

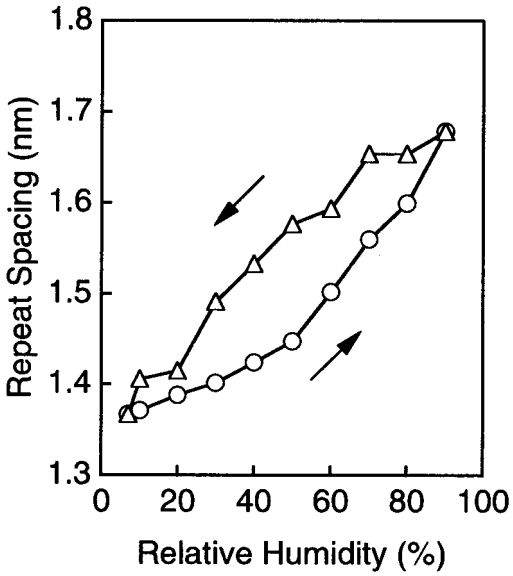

Figure 6. Relative humidity dependence of the multilayer repeat distance for the film of PEI/$Ti_{1-\delta}O_2^{4\delta-}$/(PDDA/$Ti_{1-\delta}O_2^{4\delta-}$)$_9$. Cycles and triangles represent the humidification and drying process, respectively. The film was equilibrated at each humidity for 1 h before measurements.

study took much longer (more than 1 h) to be equilibrated with surrounding moisture. This difference may be associated with the chemical nature of the nanosheet crystallites. The titania nanosheet has a higher charge density than smectite clay minerals,[19] which consequently gives a higher hydration energy.

To understand the crystalline degree of the multilayer assembly, X-ray diffraction (XRD) profiles were simulated for a system of ($Ti_{1-\delta}O_2^{4\delta-}$/PDDA)$_{10}$. The absence of higher order lines as well as the markedly broad 010 peak suggest a deviation from the regular one-dimensional sequence. Thus, a structural disorder is introduced by assuming some Gaussian spread of the multilayer repeat distance around its average of 1.5 nm. The profiles were simulated for various values of its standard deviation (α) by eq 2, and the results for the case of the multilayer assemblies of 10 bilayers are shown in Figure 7. The top pattern corresponds to one without any disorder. By the introduction of a higher degree of irregularity (larger value of α), the diffraction lines become broader, which is more significant for higher order reflections. The standard deviation of 0.3 nm gives a profile similar to the observed data (Figure 5a). The full width half-maximum (fwhm) of the 010 peak, 1.8°, is comparable to the observed value of 1.9°. In addition, higher order reflections become too broad to be recognized as peaks. The α value of 0.3 nm reaches 20% of the average multilayer stacking spacing of 1.5 nm. To visualize the degree of structural disorder, the nanosheet distribution from a certain one is plotted in Figure 8. Nanosheet positions become fuzzy up to 6−7 repetitions, showing that all of the nanosheets are not fully coherent with each other. The flexible polycation and possible different hydration states between different galleries may be responsible for this degree of order, which may be inherent for multilayer systems with polymers. Actually, AFM images for the multilayer films

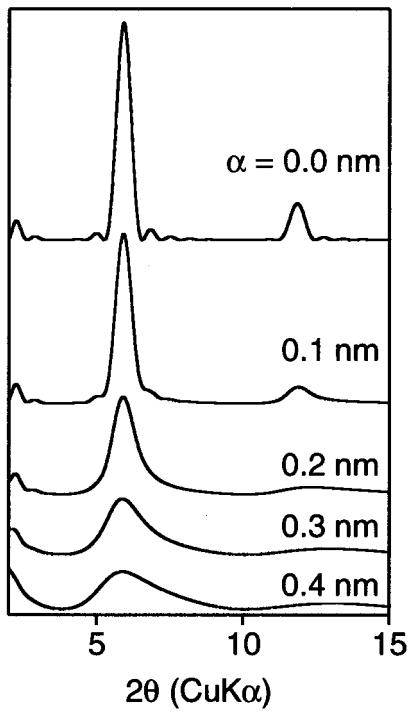

Figure 7. Calculated XRD profiles for the multilayer assemblies of (PDDA/$Ti_{1-\delta}O_2^{4\delta-}$)$_{10}$ having different degrees of disorder.

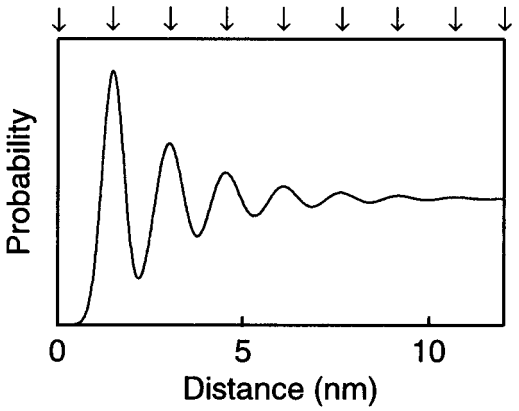

Figure 8. Spatial distribution of the nanosheets in the multilayer film of n = 10. Arrows at the top indicate the nanosheet positions at an interval of 1.5 nm for a perfectly ordered film.

revealed fuzzy features, which may indicate that the nanosheets and polycations are not perfectly oriented parallel to the substrate but are more or less crumpled. Analyses of X-ray reflectivity have been reported for several inorganic/organic multilayer films, which also revealed a heavy disorder as indicated by the rapid dumping of reflectivity due to a large surface roughness.[4c,e]

Ellipsometric Characterizations. Figure 9 shows the typical spectroscopic ellipsometry data for the multilayer film of PEI/$Ti_{1-\delta}O_2^{4\delta-}$/(PDDA/$Ti_{1-\delta}O_2^{4\delta-}$)$_9$ on Si wafer. Optical constants for the substrate were deduced by performing spectroscopic scans of a Si wafer cleaned by the same procedure and fitting the data to dispersion models for Si(100)[20] and its surface oxide. The best result for the native oxide layer was obtained by

(19) The charge density for the titania nanosheet is 3.11 nm^{-2} while that for the smectite clay sheets is typically ~1 nm^{-2}.[25,28]

(20) Jellison, G. E., Jr. *Opt. Mater.* **1992**, *1*, 47.

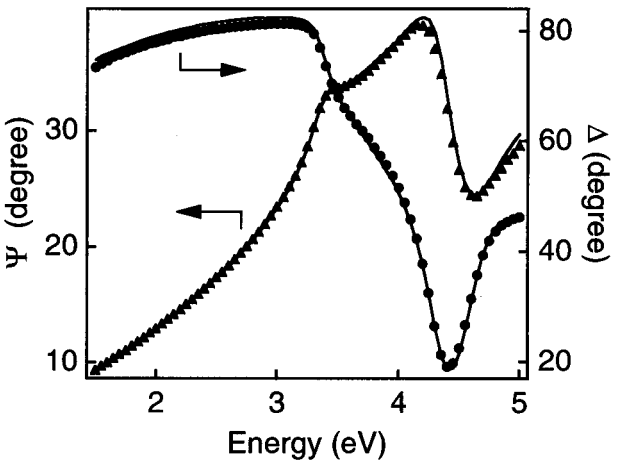

Figure 9. Spectroscopic ellipsometry scan for the multilayer film of PEI/$Ti_{1-\delta}O_2^{4\delta-}$/(PDDA/$Ti_{1-\delta}O_2^{4\delta-}$)$_9$ on Si wafer. Observed and fit data are shown as symbols and lines, respectively.

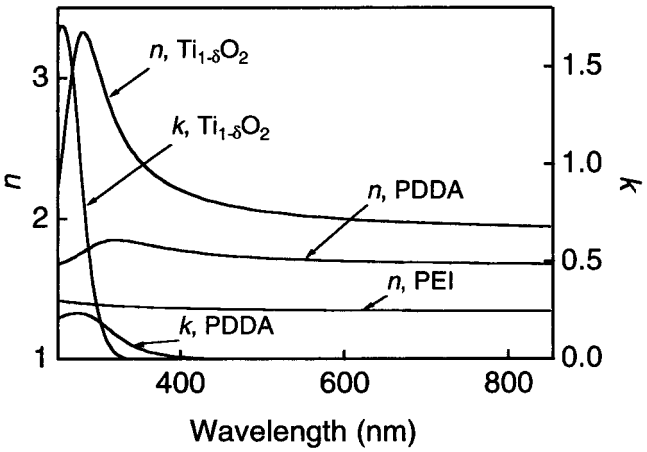

Figure 10. Optical constants for titania nanosheets and polycations as a function of wavelength.

an effective medium model where 6% of voids is included in the SiO_2 matrix that is 2.0 nm thick. The optical constants for the film components such as PEI, $Ti_{1-\delta}O_2^{4\delta-}$, and PDDA were also separately derived with samples of substrate/PEI, substrate/PEI/$Ti_{1-\delta}O_2^{4\delta-}$, and substrate/PEI/$Ti_{1-\delta}O_2^{4\delta-}$/PDDA, respectively. The classical dispersion formula was used to model the polycations while a dispersion relation based on quantum mechanical theory was employed for $Ti_{1-\delta}O_2^{4\delta-}$.[21] The PEI thickness was determined as 0.80 nm. The obtained refractive indices and extinction coefficients are plotted as a function of wavelength (see Figure 10). The extinction coefficients were zero for all the film components in a visible light region, being consistent with its good transparency. The refractive index for $Ti_{1-\delta}O_2^{4\delta-}$ (2.00 at 600 nm) is small for titanium oxide. On the contrary, the PDDA layer has a relatively large *n* (1.70 at 600 nm) for organic substances.[22] This may be attributable to positional fluctuation of the nanosheet and polycation layers from the substrate surface, which is likely to occur on a length scale of the ellipsometry probe (0.5 mmϕ) because of more or less incoherent topography of a film associated with a finite lateral size of the nanosheets. This situation may be strictly analyzed by introducing an intermediate layer in addition to those of pure $Ti_{1-\delta}O_2^{4\delta-}$ and PDDA. However, this calculation needs more parameters to be refined, which is difficult to converge. The approximation with the optical constants above for $Ti_{1-\delta}O_2^{4\delta-}$ and PDDA is more practical for modeling the system with a reasonable number of parameters.

In the final fitting process of the multilayer film composed of 10 layer pairs, only thickness parameters of $Ti_{1-\delta}O_2^{4\delta-}$ and PDDA were refined keeping the others fixed because of severe correlation between some parameters.[23] The refinement yielded the thicknesses of 1.19 ± 0.02 and 0.67 ± 0.04 nm for layers of $Ti_{1-\delta}O_2^{4\delta-}$ and PDDA, respectively, which gives a total film thickness of 18.6 nm. The titania-nanosheet thickness agrees well with the thickness data from the AFM height profile but is larger than a crystallographic thickness for the nanosheet crystallite (~0.70 nm).[13,15] This difference may be ascribed to the water molecules adsorbed on its surface, which has been discussed elsewhere.[15] Furthermore, their sum, 1.86 nm, is close to the multilayer repeat distance of 1.7 nm determined by XRD for the film immediately after the preparation.

Experimental Section

Reagents and Materials. Reagents such as Cs_2CO_3 and TiO_2 were of 99.99% purity or higher (Rare Metallic, Co.). PEI and PDDA chloride were purchased from Aldrich Co. as 50 and 10 wt % aqueous solutions, respectively, and used without further purification. The molecular weight was $\sim 7.5 \times 10^5$ for PEI and $\sim(1-2 \times 10^5)$ for PDDA. All the other chemicals were of analytical grade. All water used was purified to a resistivity of >17 MΩ cm by a Milli-Q reagent water system.

A layered titanate $Cs_{0.7}Ti_{1.825}\square_{0.175}O_4$ (□: vacancy) was prepared by solid-state calcination of an intimate mixture of Cs_2CO_3 and TiO_2 (1/2.65 in molar ratio) at 1073 K for 40 h.[24,25] Interlayer Cs ions were removed by treating the Cs−titanate powder (~70 g) with 2 dm^3 of a 1 mol dm^{-3} HCl solution for 3 days. The HCl solution was renewed each day to ensure complete exchange.

Exfoliation. The acid-exchanged phase (0.4 g), $H_{0.7}Ti_{1.825}\square_{0.175}O_4 \cdot H_2O$, was agitated vigorously with 100 cm^3 of a TBAOH solution at ambient temperature.[12] The TBA concentration was 0.017 mol dm^{-3}, and these conditions give an equivalent stoichiometry of the agent with respect to the exchangeable protons in $H_{0.7}Ti_{1.825}\square_{0.175}O_4 \cdot H_2O$, which is favorable for delamination into single sheets. When the mixture was shaken for 10 days, it yielded a turbid colloidal suspension in which the unilamellar crystallites of $Ti_{1-\delta}O_2^{4\delta-}$ ($\delta \sim 0.09$) were dispersed.

Fabrication of Multilayer Ultrathin Films. Quartz glass platelets, Si wafers, and mica chips, 1×5 cm^2 in size, were used as substrates. The former two were cleaned by being immersed in a bath of 1/1 methanol/HCl and concentrated H_2SO_4 for 30 min each. Mica was peeled off in water to have a fresh surface. The substrates were primed by being treated with a PEI solution (2.5 g dm^{-3}) for 20 min to introduce the positive charge to the substrate surface.

(21) (a) Forouhi, A. R.; Bloomer, I. *Phys. Rev. B* **1986**, *34*, 7018. (b) Forouhi, A. R.; Bloomer, I. *Phys. Rev. B* **1988**, *38*, 1865.

(22) The refractive index for TiO_2 is 2.616 for rutile and 2.554 for anatase (at 589 nm) while those for organic compounds are mostly 1.3−1.5. Cited from the *Handbook of Chemistry and Physics*, 55th ed.; Weast, R. C., Ed.; CRC Press: Cleveland, 1974.

(23) The refinements were carried out under constraints that each layer of $Ti_{1-\delta}O_2^{4\delta-}$ and PDDA should have the same thickness.

(24) (a) Hervieu, M.; Raveau, B. *Rev. Chim. Miner.* **1981**, *18*, 642. (b) Grey, I. E.; Li, C.; Madsen, I. C.; Watts, J. A. *J. Solid State Chem.* **1987**, *66*, 7.

(25) (a) Sasaki, T.; Komatsu, Y.; Fujiki, Y. *Chem. Commun.* **1991**, 817. (b) Sasaki, T.; Watanabe, M.; Michiue, Y.; Komatsu, Y.; Izumi, F.; Takenouchi, S. *Chem. Mater.* **1995**, *7*, 1001.

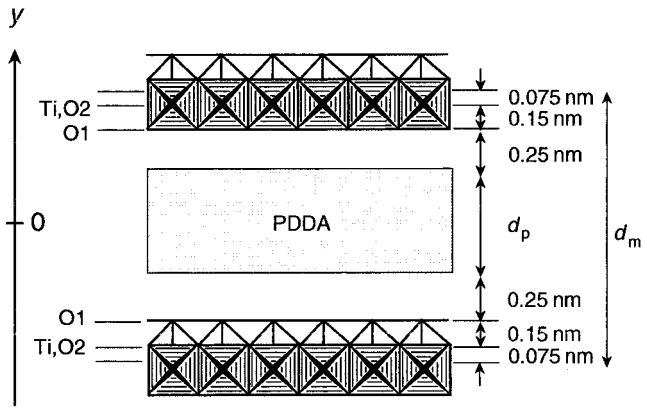

Atom	*n*	*y*
Ti	0.9125	$\pm(d_m/2 - 0.075)$
O1	1	$\pm(d_m/2 - 0.225)$
O2	1	$\pm(d_m/2 - 0.075)$
PDDA	$d_p/2.0$	$-d_p/2 \sim +d_p/2$ (continuous)

Figure 11. Structural model for the multilayer assembly of titania nanosheets and PDDA. Positional parameters for the titania nanosheets are derived from the ideal structure.

The titania colloidal suspension (0.02−0.16 g dm^{-3}) and the PDDA solution (20 g dm^{-3}) were added with an appropriate amount of HCl or TBAOH solutions, respectively, to adjust their pH to 9. Deposition cycles of the following four steps were repeated for a desired number of times to obtain a film: (i) immersion of the substrate in the titania suspension for 5−90 min, (ii) thorough washing with water, (iii) immersion in the PDDA solution for 20 min, and (iv) rinsing with water.

Instrumentation and Measurements. UV−vis absorption spectra were recorded with a Hitachi U-4000 spectrophotometer equipped with an integrating sphere detection system. Reflectance spectra were measured with a homemade instrument. The incident beam was aligned normal to the sample, and reflected intensity was detected with a photomultiplier at an angle of 5° with respect to the incident beam.

XRD data were collected by a Rigaku Rint 2000S powder diffractometer with graphite-monochromated Cu Kα radiation (λ = 0.154 05 nm).

A Seiko instrument SPA400 AFM system was used to examine the surface topography of the films prepared on Si wafer or mica. AFM images were acquired in tapping mode with silicon tip cantilevers with a force constant of 20 N cm^{-1}.

Ellipsometric measurements were performed by a Jovin−Ybon UVISEL/DH10 spectroscopic ellipsometer equipped with a photoelastic modulator and a 75 W Xe lamp as a light source. The ellipsometric parameters, ψ and Δ in eq 2 below, were measured over a wavelength range of 240−830 nm at a fixed incident angle of 75°

$$\tilde{r}_p/\tilde{r}_s = (\tan\psi)e^{i\Delta} \quad (2)$$

where $\tilde{r}_p$ and $\tilde{r}_s$ are the complex amplitude reflection coefficients for p- and s-polarized light, respectively.

Simulations of XRD Profiles. XRD profiles were simulated for a multilayer model of *N* parallel titania nanosheets in which the intersheet distance of d_m shows Gaussian distribution. The diffraction from this system can be formulated as below.[26]

$$I(\theta) = \frac{F^2(\theta)}{N}\left[N + 2\sum_{n=1}^{N-1}(N-n)e^{-8\pi^2 n\alpha^2\sin^2\theta/\lambda^2}\cos(4\pi n d_m \sin\theta/\lambda)\right] \quad (3)$$

where θ and λ are the scattering angle and wavelength of X-ray, respectively. The parameter, α, is the standard deviation of Gaussian distribution which is introduced as a measure of structural disorder. The structure factor, $F(\theta)$, was calculated by the following equation based on a nanosheet/polycation structural model shown in Figure 11.

$$F(\theta) = 2\int_0^{d_p/2}(f_P/2.0)\cos 2\pi(2y\sin\theta/\lambda)dy + 2\times 0.9125 f_{Ti}\cos 2\pi[2(d_m/2 - 0.075)\sin\theta/\lambda] + 2f_O\cos 2\pi[2(d_m/2 - 0.225)\sin\theta/\lambda] + 2f_O\cos 2\pi[2(d_m/2 - 0.075)\sin\theta/\lambda] \quad (4)$$

where f_{Ti}, f_O, and f_P are atomic scattering factors for the Ti and O atoms,[27] and a virtual atomic species comparable to PDDA, respectively. Since the structure is centrosymmetric with respect to $y = 0$, sine terms can be neglected.

The X-ray scattering of PDDA was modeled as a uniform electron density of thickness, d_P. This approximation may be valid since PDDA in various configurations should give a continuous electron density in projection parallel to the nanosheet gallery. One imaginary entity having an average scattering amplitude of PDDA, $C_8H_{16}N$, was included per 4.6 Ti atoms, which is based on the compositional data for a PDDA/titanate nanocomposite, $(PDDA)_{0.4}H_{0.3}Ti_{1.825}\square_{0.175}O_4\cdot 0.7H_2O$, synthesized in bulk.[18]

Acknowledgment. The authors are grateful to Dr. Yoshiki Wada of Advanced Materials Laboratory, National Institute for Materials Science, for his assistance in the measurements of reflectance spectra.

CM010478H

(26) Reynolds, Jr., R. C. *Modern Powder Diffraction*; Bish, D. L., Post, J. E., Eds.; The Mineralogical Society of America: Washington, DC, 1989; pp 159−163.

(27) *International Tables for Crystallography*; Wilson, A. J. C., Prince, E., Eds.; The International Union of Crystallography, Kluwer Academic Publishers: Dordrecht/Boston/London, 1999; Vol. C.

(28) *Crystal Structures of Clay Minerals and Their X-ray Identification*; Brindley, G. W., Brown, G., Eds.; Mineralogical Society: London, 1980.